Quantitative Histology and MGF Gene Expression in Rats following SSC Exercise *In Vivo*

BRENT A. BAKER, K. M. K. RAO, ROBERT R. MERCER, KEN B. GERONILLA, MIKE L. KASHON, GERALD R. MILLER, and ROBERT G. CUTLIP

National Institute for Occupational Safety and Health, Health Effects Laboratory Division, Morgantown, WV

ABSTRACT

BAKER, B. A., K. M. K. RAO, R. R. MERCER, K. B. GERONILLA, M. L. KASHON, G. R. MILLER, and R. G. CUTLIP. Quantitative Histology and MGF Gene Expression in Rats following SSC Exercise *In Vivo*. *Med. Sci. Sports Exerc.*, Vol. 38, No. 3, pp. 463–471, 2006. **Purpose:** We investigated the effects of muscle length during stretch-shortening cycles (SSC) *in vivo* on changes in MGF gene expression and quantitative morphometry in rat skeletal muscle. **Methods:** Dorsiflexor muscles of male Sprague–Dawley rats were exposed to seven sets of 10 SSC at $500^{\circ}\cdot s^{-1}$. Animals were randomly assigned to a long muscle length injury group (L-inj), short muscle length injury group (S-inj), or isometric group (Iso), with recoveries examined at 6 or 48 h post-injury for each group. Following exposure, animals were euthanized, and the tissue was prepared for either histology (quantitative morphometry) or RNA isolation, followed by quantitative real-time reverse transcriptase polymerase chain reaction. mRNA levels were measured for mechano-growth factor (MGF), while 18S ribosomal RNA served as the internal reference sample. **Results:** Stereological measures indicative of edema and myofiber degeneration were significantly increased in the L-inj SSC group at 48 h when compared with the S-inj or Iso group. MGF mRNA was increased transiently at 6 h in the isometric group. In contrast, MGF mRNA was increased at 48 h in the S-inj, but was not increased at either time point in the L-inj group. **Conclusion:** These data strongly indicate that exposure to SSC at longer muscle lengths result in greater morphometric indices of inflammation and degeneration than SSC conducted at a shorter muscle lengths or isometric contractions, at the same time that the adaptation to SSC was prolonged and, apparently, not resolved in the L-inj group that was manifested by the lack of up-regulation in MGF mRNA. **Key Words:** MUSCLE INJURY, STRETCH-SHORTENING CYCLES, STEREOLOGY, mRNA EXPRESSION

Resistance-type exercise is characterized by multiple, dynamic elements that influence the response of skeletal muscle. Repetitive muscular contractions, or stretch-shortening cycle (SSC) contractions, may lead to skeletal muscle adaptation (regeneration and growth) or maladaptation (inflammation, degeneration, and dysfunction); however, none of these processes are likely to be mutually exclusive. In most cases, muscles compensate for increased demands in a systematic fashion, yet situations do arise in which the muscle does not adequately meet those demands. It has been demonstrated that contractions occurring while the muscle is lengthening, not shortening or isometric contractions, produce injury (12,19,27), functional impairments (4,9,29), or morphological changes (7,18). However, the model and target muscle used to investigate myofibrillar changes following injurious contractions have varied (1,7,9,18).

Address for correspondence: Robert G. Cutlip, Ph.D., 1095 Willowdale Road, MS L-2027, Morgantown, WV 26505; E-mail: rgc8@cdc.gov.
Submitted for publication February 2005.
Accepted for publication August 2005.

0195-9131/06/3803-0463/0
MEDICINE & SCIENCE IN SPORTS & EXERCISE®

DOI: 10.1249/01.mss.0000191419.67030.69

Numerous mechanical factors have been shown to affect the magnitude of injury to skeletal muscle following repetitive muscular contractions (4). One important factor is muscle length, which has been associated with contraction-induced muscle injury incurred during exercise (4,9). Single eccentric contractions (12) have been used to investigate muscle damage; however, the muscle lengths used were significantly outside the physiological range of the target muscle. Thus, multiple contractions are necessary under controlled loading conditions when inducing muscle injury *in vivo* within the physiological range, and this may further enhance the external validity of such findings when compared with single-stretch paradigms. Furthermore, it is during activities such as those observed in athletic and occupational settings that skeletal muscle encounters periods of alternating, repetitive lengthening and shortening contractions along with periods of isometric contractions. Therefore, it is necessary to develop physiologically relevant models when studying skeletal muscle *in vivo* that reflect such changes (4,8,14). Accordingly, SSC are an appropriate model to study muscle injury *in vivo* (14). SSC have been shown to lead to significant myofiber degeneration (7) as well as an increased cellular interstitial response, indicative of cellular infiltrates (2). The role of muscle length in adaptation to skeletal muscle injury has been widely studied (4,9,12,28), and the results obtained from functional profiling illustrate that exposure to active excursions at longer muscle lengths lead to greater

muscle damageand force deficits than active excursions at shorter muscle lengths or isometric contractions (4,9). While skeletal muscle offers one of the best cases to study tissue adaptability, quantitative morphometric data are scarce; this is primarily due the difficulty in quantifying inflammatory and degenerative processes by light microscopy (2). In addition, since stretch combined with electrical muscle stimulation has been shown to be a powerful stimulus for changes in gene expression (autocrine and/ or paracrine), investigation of local factors may be beneficial in understanding the adaptation process. Recently, Goldspink and colleagues (10,11,20) have elucidated the role of a local form of IGF-1 in animals and humans, which is produced by the myofiber and activated satellite cells. This isoform is alternatively spliced from the mature IGF-1 gene (16,23), known as IGF1-Eb (in rats), and has been shown to be activated by electrical stimulation and mechanical stretch and designated mechano-growth factor (MGF). Furthermore, Hill and colleagues (11) have proposed a role for MGF in initiating satellite cell activation in response to local tissue damage. Moreover, muscle-specific genes that are influenced by mechanical stimuli may be more indicative of the ongoing local adaptation response following exposure to exercise (SSC) than systemic factors. This concept is very important, since adaptation, positive and/or negative, occurs in the specific region/muscle perturbed. Even though it is well recognized that exposure to injurious contractions results in inflammation as well as myofiber degeneration (3), there is still not a thorough understanding of the impact that different muscle lengths have on the relationship between inflammation, myofiber degeneration, and regenerative changes in gene expression.

Our purpose was to study the changes in muscle morphology using a standardized stereological technique and concurrently measure changes in MGF gene expression using real-time quantitative reverse transcriptase polymerase chain reaction (RT-PCR) in rat skeletal muscle exposed *in vivo* to SSC exercise of varying muscle lengths. The functional data were collected on these animals and published previously (4). Those data indicated that SSC conducted at longer muscle lengths resulted in a more pronounced force deficit than isometric contractions or SSC conducted at shorter muscle lengths. Based on those findings, we hypothesized that SSC at a longer muscle length will also result in greater quantitative morphometric indices of inflammation and degeneration than SSC conducted at a shorter muscle length or isometric contractions. Additionally, we hypothesized that SSC conducted at a longer muscle length will result in increased levels of mRNA expression for MGF, as opposed to SSC conducted at a shorter muscle length or isometric contractions.

METHODS

Animal Handling

Male Sprague–Dawley rats (N = 36) were selected for use in the present study (446 ± 32 g, 12 wk of age) and were housed in an Association for Assessment and Accreditation of Laboratory Animal Care–accredited (AAALAC) approved animal quarters. Temperature and light/dark cycle (dark cycle from 7:00 a.m. to 7:00 p.m.) were held constant for all animals; food and water were provided *ad libitum*. After 1 wk of acclimatization, all animals were subjected to a standardized experimental protocol approved by the National Institute for Occupational Safety and Health Animal Care and Use Committee before conducting the experimental protocols. Animals were randomly assigned to an isometric group with 6 h of recovery (N = 6) or 48 h of recovery (N = 6); a short muscle length injury group with 6 h of recovery (N = 6) or 48 h of recovery (N = 6); or a long muscle length injury group with 6 h of recovery (N = 6) or 48-h recovery (N = 6).

Experimental Setup

Rats were tested on a custom-built rodent dynamometer (Fig. 1A) (5). A Labview-based virtual instrument was developed that governed a National Instruments data acquisition board (PCI-MIO-16XE-10) and Unidex 100 motion controller (Aerotech Inc., Pittsburgh, PA) for precise control of a brushless DC servomotor (1410 DC, Aerotech Inc.) and muscle stimulator (Model SD9, Grass Medical Instruments, Quincy, MA). The software also acquired and stored position, force, and velocity data in real time as described below. The animal setup was similar to one described previously by Cutlip and colleagues (4). Briefly, rats were anesthetized with isoflurane gas using a small animal anesthetic system (Surgivet Anesco Inc.). On the basis of contractile performance, stable ventilatory rates, and fast induction and recovery times, this class of anesthetic agent is an appealing choice as an anesthetic for either acute or long-term studies examining skeletal muscle function. First, rats were placed in an "induction" tank-filled with a mixture of isoflurane gas and oxygen. Then, each rat was placed supine on the heated x–y positioning table of the rodent dynamometer, with an anesthetic mask placed over its nose and mouth. The knee was secured in flexion (at 90°) with a knee holder. The left foot was secured in the load cell fixture using a custom-built foot holder with the ankle axis aligned with the axis of rotation of the load cell fixture. Each animal was monitored during the protocol to ensure proper anesthetic depth and body temperature.

Exercise Testing

The joint position of the animal was defined by the angle between the tibia and the plantar surface of the foot. The angular position of the load cell fixture corresponded with the angular position of the ankle. Vertical forces applied to an aluminum sleeve fitted over the dorsum of the foot were translated to a load cell transducer (Sensotec, Inc.) in the load cell fixture. The force produced by the dorsiflexor muscles (consisting of the tibialis anterior (TA) and extensor digitorum longus (EDL)) was measured at the interface of the aluminum sleeve and the dorsum of the

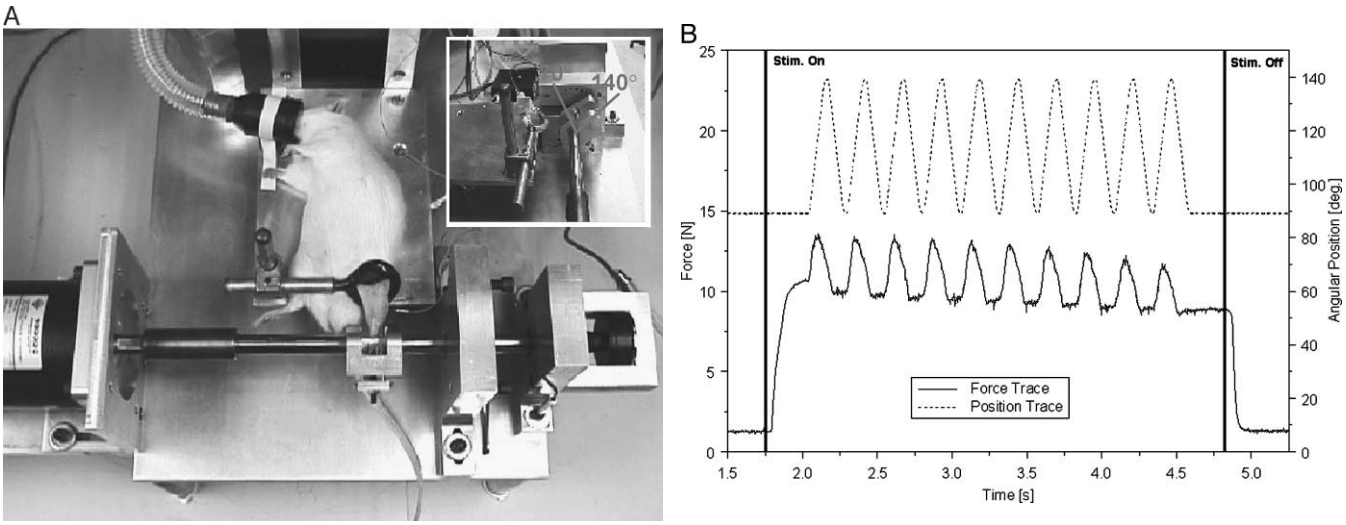

FIGURE 1—A. Experimental setup, including dynamometer with exercise test (aerial view) and dynamometer with joint angles (lateral view). B. Typical force trace, angular position trace, and electrical stimulation timing of one set of 10 stretch-shortening contractions.

foot (Fig. 1A). Platinum stimulating electrodes (Grass Medical Instruments) were placed subcutaneously to span the peroneal nerve. Activation of the electrical stimulator resulted in muscle contraction of the dorsiflexor muscle group. Stimulator settings were optimized based on pilot studies to maximize dorsiflexor isometric force using a supramaximal stimulus. A supramaximal stimulus was used to ensure all motor units were fully activated during the exercise testing protocol. Muscle stimulation for all protocols was a 120-Hz square wave pulse at 0.2-ms pulse duration, and 4 V. To reduce the effect of fatigue, all electrical stimulation times were kept to a minimum with recovery times between stimulations.

Injury Protocol

Two groups were exposed to an injury protocol that consisted of stretch-shortening contractions. Each group received 70 stretch-shortening contractions induced at a range of motion at either 70–120° (S-inj) or 90–140° (L-inj). The ranges of motion selected were based on multipositional isometric testing of the rat dorsiflexors as described in Cutlip et al. (4). Isometric forces increased from a joint angle of 70° to approximately 100° before reaching a plateau and decreasing as the joint angle increased to 140°. In this model, the maximum joint excursion occurs at 140° plantar flexion and 70° dorsiflexion (before interference of the load cell with the tibia). Furthermore, the dorsiflexor muscle length in the current investigation is based on a 90° ankle–joint angle. In this position, dorsiflexor muscle length is optimal for the isometric group, while the S-inj and L-inj groups initiate movement at an optimal position on the length-tension curve and conclude on the descending portion of the length–tension curve based on data by Ledvina and Segal (15). The stretch-shortening contractions were induced by fully activating the dorsiflexor muscles for 100 ms and then moving the load cell fixture in the prescribed range of motion at a velocity of $500°\cdot s^{-1}$. This occurred in a reciprocal fashion for 10 oscillations (this required 2.4 s due to motor ramp up and ramp down times). After 10 immediately successive oscillations were complete, the load cell fixture was stopped and the dorsiflexor group was deactivated 300 ms later (Fig. 1B). The total stimulation time per set was 2.8 s. The seven sets of 10 oscillations were conducted at 1-min intervals.

Isometric Protocol

The Iso group was exposed to seven noninjurious, maximal isometric contractions conducted at 1-min intervals. During each contraction, dorsiflexor muscles were stimulated for duration of 2.8 s at an ankle angle of 90° using the same stimulation parameters and duration as in the two injury groups. This served as a non injury, metabolic control.

Tissue Processing and Histology

At 6- or 48-h recovery following the SSC, rats were weighed, anesthetized with sodium pentobarbital (ip, $10\ mg\cdot100\ g^{-1}$ body weight) and exsanguinated. Following excision, processing of tissue occurred immediately. The left ($N = 36$) and right ($N = 36$) TA muscles were dissected, cleaned, and weighed. Each muscle was cut transversely and allocated for histology or RNA isolation. First, the midbelly was cut from each muscle and mounted on cork, immersed in optimal cutting temperature compound, frozen in isopentane cooled with liquid nitrogen, and stored at −80°C. The midbelly region was selected to obtain the maximum tissue sample, since it may be likely that all the

TABLE 1. Sequence of the specific sets of primers that were used in RT-PCR analyses.

Gene	Primers	Product (Base Pairs)
MGF	Sense: TCC GCT GCA AGC CTA CAA AGT C Antisense:- CTT TCC TTC TCC TTT GCA GCT TCC	126
18 S rRNA	Sense: GGA CCA GAG CGA AAG CAT TTG C Antisense: CGC CAG TCG GCA TCG TTT ATG	115

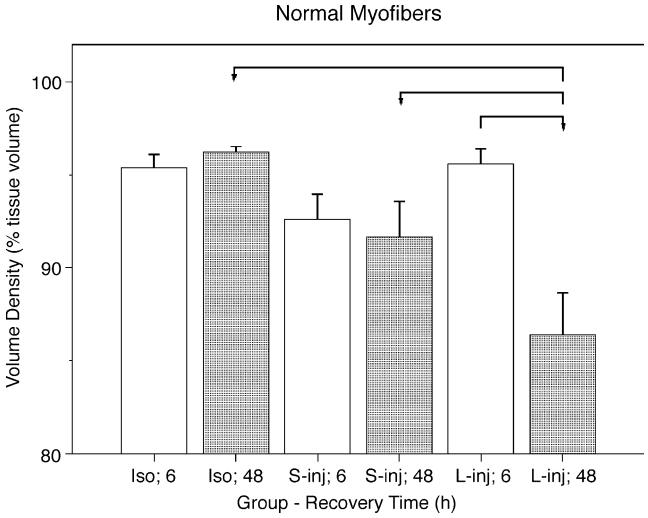

FIGURE 2—The percentage of volume density of normal myofibers of muscles exposed to SSC of varying muscle lengths. SSC of varying muscle lengths altered the response of the normal myofiber percentage of volume density by decreasing the percentage of volume density of normal myofibers in the L-inj compared with the Iso and S-inj groups at 48 h (treatment effect at 48 h: L-inj < Iso, L-inj < S-inj). In addition, there was a decrease in the normal myofiber volume density in the L-inj group (time effect: 48 h < 6 h). Group (N = 6) data shown are mean values ± SEM.

fibers in this muscle do not extend over the entire length of the muscle (6,24). Later, transverse sections (12 μm) were cut, mounted on precoated microscope slides (N = 36, left TA), which were air dried, and stained using a routine procedure with Harris hematoxylin and eosin. Permount was used to attach coverslips to microscope slides. Tissue sections were evaluated on a Leica DMLB microscope. Next, the proximal one fourth of the left TA (exposed limb, N = 36) and right TA (contralateral control, N = 36) muscle from each animal was immersed in phosphate-buffered saline (PBS) in a micro centrifuge tube, frozen immediately in isopentane cooled in liquid nitrogen, and stored at −80°C. Because TA muscle fibers may not extend the entire length of the muscle, and the fibers that terminate intramuscularly potentially may be involved in the regenerative process, using the proximal portion relative to the muscle midbelly of the TA for molecular analysis is appropriate (30).

Myofiber Definitions

The methodological techniques have been described in detail by Baker and colleagues (2). Briefly, stereology was used to quantify the degree of myofiber degeneration, and the accompanying changes in the interstitial space in the TA muscle from each group. Myofibers were defined by the following criteria: normal myofibers demonstrated 1) complete contact with adjacent myofibers, 2) a smooth outer membrane, and 3) no presence of internal inflammatory cells. Degenerative myofibers displayed 1) a loss of contact with adjacent myofibers, 2) the presence of internal inflammatory cells, and 3) an outer membrane interdigitated with inflammatory cells.

Stereology

Quantitative morphometric methods were used to measure the volume density, surface densities, and average thickness of normal myofibers, degenerative myofibers, and the interstitial space. Briefly, the interstitium was divided into the endomysium and the perimysium space, which included capillaries. Stereology was also used to quantify the degree of inflammation, which was quantified as either noncellular interstitium (NCI), indicative of edema, or cellular interstitium (CI); CI consisted of all possible infiltrating cells such as, but not limited to, inflammatory, endothelial, and fibroblasts. Volume and surface density were measured using standard morphometric analyses (26), while one histological slide was used for each animal. A stage micrometer was used to identify the midpoint of the section. Point and intercept counts using a 121-point/11-line overlay graticule (12.5 mm^2 with 100 divisions) at 40× magnification were taken at five equally spaced points across the section. This process was repeated 2 mm on either side of the midpoint of the section for a total of 1210 points and 110 intercept lines per section. We addressed the possible concern for sampling in previous methodological work (data not published) in which we initially sampled five fields (605 points and 55 intercept lines per section). By doubling the sampling fields to 10 (2), we observed no further decrease in our coefficient of variation. Volume density or percent volume was computed from the percentage of total points over the tissue section to points over each: normal myofibers, degenerative myofibers, CI, and NCI plus capillaries. Intercepts over the line overlay were counted for the perimeter of normal myofibers, degenerative myofibers, and interstitium to myofiber transitions. Points and intercepts over blood vessels >25 μm in diameter were excluded. Average thickness or average distance was computed from twice

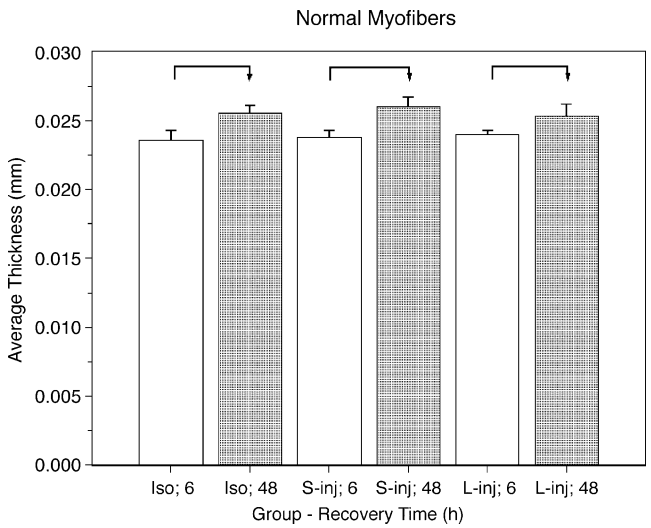

FIGURE 3—The average thickness of normal myofibers of muscles exposed to SSC of varying muscle lengths. The response of the normal myofiber's average thickness was increased following exposure to SSC at 48 h compared with 6 h (time effect in all groups: 48 h > 6 h). Group (N = 6) data shown are mean values ± SEM.

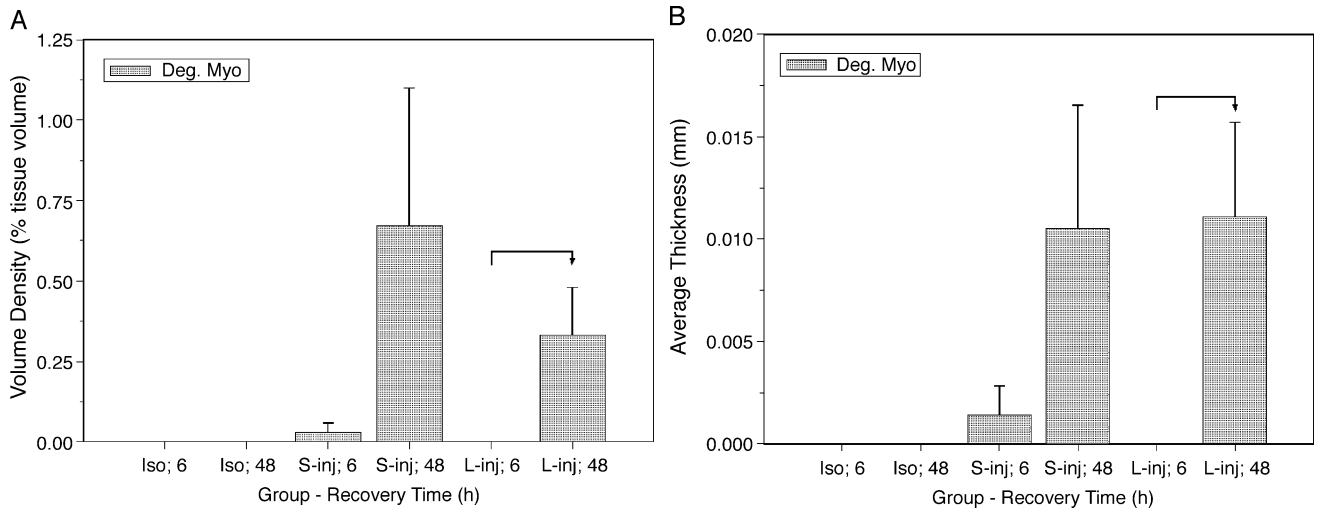

FIGURE 4—A. The percentage of volume density of degenerative myofibers of muscles exposed to SSC of varying muscle lengths. SSC significantly altered the percentage of volume density of degenerative myofibers over time in the L-inj group only (time effect: 48 h > 6 h). Group ($N = 6$) data shown are mean values ± SEM. B. The average thickness of degenerative myofibers of muscles exposed to SSC of varying muscle lengths. The L-inj group's degenerative myofiber thickness was significantly increased at 48 h (time effect: 48 h > 6 h). Group ($N = 6$) data shown are mean values ± SEM.

the ratio of volume-to-surface density according to standard morphometric analysis (26). One section per animal, with six animals per group, was evaluated, and the results expressed as mean ± SEM.

Gene Expression

RNA isolation. A 50- to 75-mg portion was cut from the frozen muscle sample allocated for gene expression, immediately immersed in lysis buffer (Catalog #072R31A, Qiagen, Valencia, CA), and minced with a razor blade. Samples were solubilized directly in lysis buffer using a mini bead beater (#3110BX, Bio-Spec Products Inc.) with 1.0-mm zirconia beads (Bio-Spec Products Inc., #11079110zx-B) per the manufacturer's instructions. Solubilized muscle sample was transferred to a clean micro centrifuge tube and stored at −80°C to await total RNA isolation. RNeasy Mini Kits (Qiagen, #74106) were used to isolate total RNA from solubilized muscle samples. Briefly, the solubilized muscle tissue was spun down and treated with proteinase K (Qiagen, #19133) for 20 min at 55°C. The samples were then centrifuged at 13,200 rpm, the supernatant was run through a QIA shredder (Qiagen), and the isolated RNA samples were treated with DNase-1 (Qiagen, #79254). RNA concentration was determined spectrophotometrically via optical density at 260–280 nm. The RNA samples were then frozen and stored at −80°C until used for subsequent RT-PCR procedures. All subsequent steps were carried out as described by the manufacturer's specifications (Qiagen).

RT-PCR. One to two micrograms of the DNAse I-treated RNA were reverse transcribed for each muscle sample, in duplicate, using Superscript II reverse transcriptase (#18064014, Life Technologies, Gaithersburg, MD). Subsequently, the mRNA levels were measured using a SYBR Green PCR kit with the ABI 5700 Sequence Detector (PE Applied Biosystems, Foster City, CA). Five microliters of the reverse-transcribed mixture were used to conduct the PCR reaction according to the SYBR Green PCR kit instructions. Sequences for MGF and 18S (housekeeping gene (HKG)) are shown in (Table 1). In preliminary experiments, the products were analyzed by gel electrophoresis, and a single product was obtained for each primer set. The comparative C_T (threshold cycle) method was used to calculate the relative concentrations (User Bulletin #2, ABI PRISMR 7700 Sequence Detector, PE Applied Biosystems). Briefly, the method involves obtaining the C_T values for the gene of interest, normalizing that value to a housekeeping gene (18 S in the present case), and deriving the fold increase compared to the control contralateral samples.

Statistical Analyses

Statistical analyses were conducted using SAS Version 8 (SAS Institute, Cary, NC). Stereological measurements of percentage of volume density and average thickness of cellular and noncellular components, and RT-PCR data were analyzed using two-way (treatment × time) ANOVA. Where appropriate, *post hoc* comparisons were conducted using Fisher's least significant difference tests. Data for the measurement of the percentage of volume density and average thickness of degenerative myofibers was regarded as ordinal, so a nonparametric Kruskal–Wallis test was applied, and when differences were statistically significant, a Mann–Whitney *U*-test was performed. The level of statistical significance for all analyses was set at $P < 0.05$.

RESULTS

Stereological quantification. Initially, we investigated the effects varying SSC muscle length had on stereological indices of inflammation, degeneration, and modifications occurring in the interstitial space. The percentage of volume

density of normal myofibers was not different between groups at 6 h; however, at 48 h it was significantly greater in both the Iso and S-inj SSC groups as compared with the L-inj SSC group ($P < 0.0001$ and $P < 0.014$, respectively; Fig. 2). Furthermore, there was a significant decrease in the percentage of volume density of normal myofibers at 48-h recovery compared with the 6-h recovery in the L-inj SSC group ($P < 0.0001$, Fig. 2). Indices for average thickness of normal myofibers for all groups were significantly increased at 48 h compared with 6 h ($P < 0.05$; Fig. 3).

Stereological analyses of myofiber degeneration. The percentage of volume density of degenerative myofibers increased significantly from 6 to 48 h in the L-inj SSC group only ($P < 0.05$, Fig. 4A). The average thickness of degenerative myofibers was also significantly increased in the L-inj group at 48 h ($P < 0.05$, Fig. 4B).

Stereological analyses of inflammation. The percentage of volume density of CI, indicative of cellular infiltrates, was significantly less in the Iso group when compared with the S-inj group at 6 h ($P < 0.05$) and the L-inj or S-inj group at 48 h ($P < 0.0001$ and $P < 0.05$, respectively; Fig. 5A). In addition, the percentage of volume density of the CI for the L-inj group was significantly greater at 48 h compared with 6 h ($P < 0.0001$), signifying acute inflammation (Fig. 5A). There was also a significantly increased percentage of volume density of the NCI at 48 h for the L-inj group compared with the Iso or S-inj group ($P < 0.05$ and $P < 0.05$, respectively; Fig. 5B), indicating an

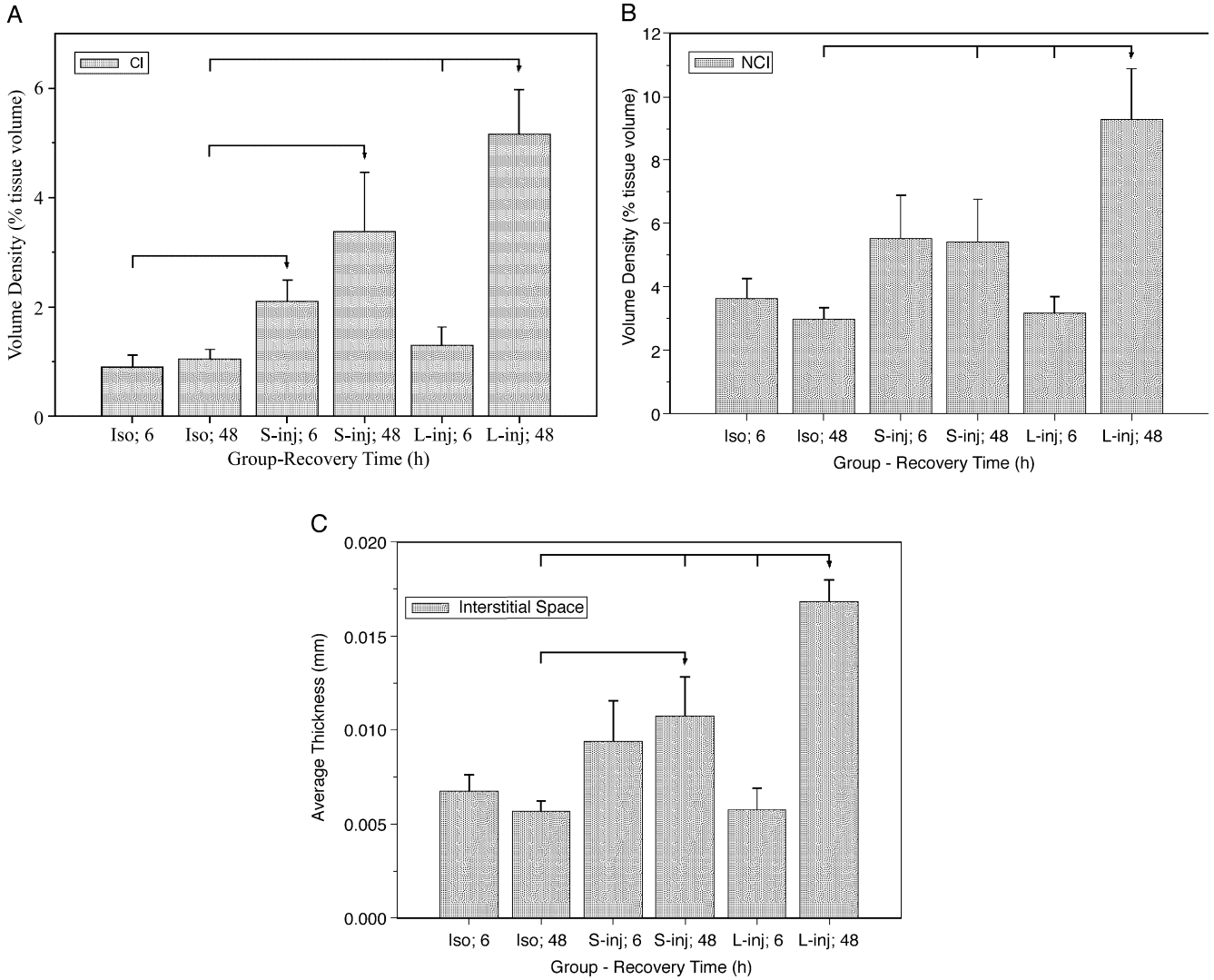

FIGURE 5—A. The percentage of volume density of CI of muscles exposed to SSC of varying muscle lengths. The volume density of the CI increased in the S-inj compared with the Iso group at 6 h (treatment effect: S-inj > Iso) and was also increased in the S-inj and L-inj groups compared with the Iso group at 48 h (treatment effect: S-inj > Iso, L-inj > Iso). However, the only increase over time was observed in the L-inj group (time effect in L-inj: 48 h > 6 h). Group ($N = 6$) data shown are mean values ± SEM. B. The percentage of volume density of NCI of muscles exposed to SSC of varying muscle lengths. SSC exposure resulted in significant NCI increases in the L-inj group compared with the S-inj and Iso groups and with respect to time (treatment effect: L-inj > Iso, L-inj > S-inj; time effect in L-inj: 48 h > 6 h, respectively). Group ($N = 6$) data shown are mean values ± SEM. C. The average thickness of the interstitial space of muscles exposed to SSC of varying muscle lengths. The interstitial space's average thickness was altered following exposure to SSC at varying muscle lengths. The S-inj group's interstitial space's average thickness was increased compared to the Iso group's interstitial average thickness at 48 h (treatment effect: S-inj > Iso). Also, the L-inj interstitial space's average thickness was increased when compared with either the Iso or S-inj group at 48 h and with respect to time (treatment effect: L-inj > Iso, L-inj > S-inj; time effect in L-inj: 48 h > 6 h, respectively). Group ($N = 6$) data shown are mean values ± SEM.

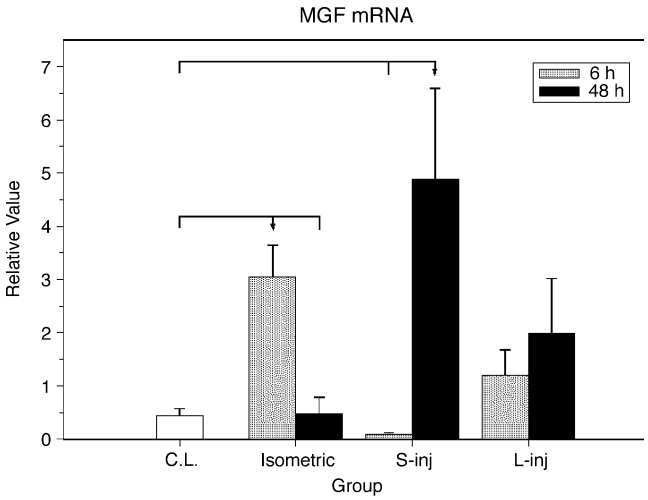

FIGURE 6—MGF mRNA levels of muscles exposed to SSC of varying muscle lengths. MGF mRNA levels were significantly increased in the Iso group at 6 h compared with the contralateral control (treatment effect: Iso > contralateral control). Additionally, the Iso group's MGF mRNA levels were significantly increased at 6 h compared with 48 h (time effect: 6 h > 48 h). Furthermore, there was a significant increase in MGF mRNA in the S-inj group at 48 h compared with the contralateral control (treatment effect: S-inj > contralateral control). Also, there was a significant increase in MGF mRNA in the S-inj group at 48h (time effect: 48 h > 6 h). Group (N = 6) data shown are mean values ± SEM.

expansion of the interstitial space that is consistent with edema. Moreover, this was the only group that demonstrated an increased NCI response from 6 to 48 h ($P < 0.05$; Fig. 5B). The average thickness of the interstitial space, which is a function of the CI and NCI, was significantly increased in the L-inj group at 48 h compared with those of the Iso or S-inj groups at the same time point ($P < 0.0001$ and $P < 0.05$, respectively; Fig. 5C). The S-inj group at 48 h also had a significantly larger interstitial space thickness when compared with the Iso group at the same time point ($P < 0.05$, Fig. 5C). Only the L-inj group showed a significantly increased average thickness in the interstitial space from 6 to 48 h ($P < 0.0001$; Fig. 5C).

Gene expression quantification. We investigated the effects that varying SSC muscle length had on the expression of MGF in the rat TA muscle. There was a significant increase in MGF mRNA in the isometric group at 6 h ($P < 0.05$; Fig. 6) and the S-inj at 48 h ($P < 0.05$; Fig. 6) relative to the contralateral control. Additionally, the Iso group's MGF mRNA levels were significantly increased at 6 h compared with 48 h (time effect: 6 h > 48 h, $P < 0.05$). Also, there was a significant increase in MGF mRNA in the S-inj group at 48 h (time effect: 48 h > 6 h, $P < 0.05$).

DISCUSSION

This is the first study, to our knowledge, that systematically quantified inflammation and myofiber degeneration by stereological analyses and the concurrent changes in MGF gene expression following a bout of SSC exercise. Specifically, we measured parameters signifying inflammation, skeletal muscle degeneration, regeneration, and modifications occurring in the interstitial space that may be influenced by variations in muscle length during an SSC exercise protocolin rats. A major finding of this study is that the SSC protocol used (70 SSC total), which previously was characterized as an adequate number of SSC for inducing myofiber degeneration (7), only produced myofiber degeneration in the L-inj group, in conjunction with the greatest increases observed in the NCI and CI. Additionally, the isometric group served as a metabolic control in this study and showed no signs of myofiber degeneration. However, the isometric group did exhibit an increased MGF mRNA response at 6 h, but this up-regulation, which occurred within such a short time frame (in the absence of degeneration) may indicate that this up-regulation is not the consequence of regenerative changes (30). In contrast, the S-inj group displayed an increase in MGF mRNA at 48 h that we interpreted as an adaptive process, since an increased CI response, indicative of celllular infiltrates, was also observed. This differential response between isometric and SSC contractions may be a function of increased intensity demands. Surprisingly, and contrary to our hypothesis, the L-inj group did not result in the greatest increase in MGF transcript levels. However, the L-inj group's SSC were composed of eccentric contractions occurring at longer muscle lengths than the two other groups, so our findings are well supported by results observed in previous studies (1,9,12,18). These investigations showed that eccentric contractions led to greater indices of skeletal muscle "disruption and damage" than those initiated at shorter muscle lengths or isometric contractions. Since the temporal response of MGF mRNA in skeletal muscle has been reported previously (11,21), the differential response we observed between the Iso, S-inj, and the L-inj groups may be due to limited sampling time points, given that MGF mRNA levels have been shown to continue to increase beyond 48 h. Alternatively, MGF mRNA has been suggested as an initiating factor in the regenerative response in cases of increased amounts of muscle injury (11,30), so an up-regulation of this gene in the L-inj in the current study may have been observed beyond 48 h. Furthermore, functional quantification of whole muscle damage, reported previously (4), revealed that exposure to SSC at long muscle lengths (L-Inj group) did indeed result in a significantly greater isometric force deficit and a slower recovery than in the S-inj or Iso group at 48 h post exposure. Thus, the absence of up-regulated MGF mRNA in the L-inj at 6 or 48 h does not appear atypical at these relatively early time points, because the inflammatory and myofiber degenerative response was most profound in this group. We do, however, acknowledge that a possible limitation in our results is that the data are reflective of the expression at the level of the gene and may not fully account for the modifications and expression observed in the MGF protein.

We recognize that using any HKG has limitations; however, in our initial studies using glyceraldehyde phosphate dehydrogenase (GAPDH) as an HKG, we observed

changes following SSC exposure (unpublished data). Obviously there is great variability in HKGs, and this variability may be influenced with different modes of exposure. Contrary to our previous observations (unpublished data), there are reports where GAPDH is suitable as a HKG (17). In addition, we measured a number of other target genes in the current investigation that did not show any change while using 18S as the HKG. Consequently, if there was a down regulation of 18S (to account for the up-regulation of MGF), then one has to assume that all the other genes measured would have been down regulated, too, a highly unlikely coincidence. Therefore, 18S is a stable HKG and thus a suitable candidate for normalizing other genes of interest in this SSC exposure protocol.

Despite the fact that the S-inj groups exhibited alterations involving its NCI and CI responses, only the L-inj group showed a significant increase in the volume density of degenerative myofibers, thus indicating acute skeletal-muscle degeneration at 48 h. Additionally, we observed a significant increase in the percentage of volume density of CI and NCI for the L-inj group at 48 h. The significant increase in the percentage of volume of degenerative myofibers, CI, and NCI at 48 h in the L-inj group indicates that exercising at longer muscle lengths results in acute inflammation as well as myofiber degeneration. However, at 6 h, we did not witness any significant noncellular or cellular responses for the two other groups, which would have indirectly reflected an increased neutrophil infiltration (22). Instead, we observed an increase in the cellular interstitium at 48 h, which has been characterized previously as an increased macrophage infiltration in the days following contraction-induced injury, specifically at 48 h (13). Since it has been hypothesized that an increase in the inflammatory response, in the absence of overt skeletal muscle "damage" may contribute to a protective effect on the exercised muscle upon subsequent exposures (22), these current findings may support that hypothesis. However, when myofiber degeneration is present, it is more likely that this protective effect would be afforded by the presence of phagocytic cell infiltration and remodeling specifically by macrophages, and not neutrophils, since regeneration of the muscle would precede functional adaptations. This may possibly delay the local growth factor response in order to cope with the initial onset of inflammation and myofiber degeneration.

Even though the protocol used in the current investigation reduced the number of repetitions by more than 50% compared with prior reported protocols (7), it induced adequate injury, as evident by the observed functional deficits (4) and morphological evidence of myofiber damage (7). Nevertheless, as the muscle length increased for each group (Iso = 90°, S-inj = 70–120°, and L-inj = 90–140°), so did the exacerbation of SSC-induced injury. For this reason, there appears to be an evident threshold that is established as the muscle length during injurious SSC exercise reaches the descending portion of the length-tension curve, which will induce myofiber degeneration and possibly the adaptation to a longer muscle length. Admittedly, the use of maximal muscle stimulation is more stressful than submaximal muscle activation; however, it is beneficial to control the activation dynamics such that the effect of changes in independent variables such as initial muscle length on muscle morphological response can be accurately studied. It has been proposed that the inflammatory process is necessary for optimal repair (25). As a result, understanding the mechanisms by which the observed cellular interstitial response influences myofiber adaptation (physiologically, molecularly, or genetically) as well as the interstitial space will provide further insight into the complex relationship between these components. Finally, these data may further our understanding as to whether local myofiber degeneration, preceded by inflammation, is a requirement for the adaptive response that is commonly observed following repeated bouts of injurious exercise.

The authors thank Dr. Ann Hubbs and Dr. Petia Simeonova of the National Institute for Occupational Safety and Health and Dr. Thomas Best of the University of Wisconsin–Madison for their critical review and comments regarding this manuscript.

REFERENCES

1. Armstrong, R. B., R. W. Ogilvie, and J. A. Schwane. Eccentric exercise-induced injury to rat skeletal muscle. *J. Appl. Physiol.* 54:80–93, 1983.
2. Baker, B. A., R. R. Mercer, K. B. Geronilla, M. L. Kashon, G. R. Miller, and R. G. Cutlip. Stereological analysis of muscle morphology following exposure to repetitive stretch-shortening cycles in a rat model. *Applied Physiology, Nutrition and Metabolism*, in press.
3. Clarkson, P. M., and S. P. Sayers. Etiology of exercise-induced muscle damage. *Can. J. Appl. Physiol.* 24:234–248, 1999.
4. Cutlip, R. G., K. B. Geronilla, B. A. Baker, M. L. Kashon, G. R. Miller, and A. W. Schopper. Impact of muscle length during stretch-shortening contractions on real-time and temporal muscle performance measures in rats in vivo. *J. Appl. Physiol.* 96:507–516, 2004.
5. Cutlip, R. G., W. T. Stauber, R. H. Willison, T. A. McIntosh, and K. H. Means. Dynamometer for rat plantar flexor muscles in vivo. *Med. Biol. Eng. Comput.* 35:540–543, 1997.
6. Edstrom, L., and E. Kugelberg. Properties of motor units in the rat anterior tibial muscle. *Acta Physiol. Scand.* 73:543–544, 1968.
7. Geronilla, K. B., G. R. Miller, K. F. Mowrey, et al. Dynamic force responses of skeletal muscle during stretch-shortening cycles. *Eur. J. Appl. Physiol.* 90:144–153, 2003.
8. Goldspink, G. Gene expression in muscle in response to exercise. *J. Muscle Res. Cell. Motil.* 24:121–126, 2003.
9. Gosselin, L. E., and H. Burton. Impact of initial muscle length on force deficit following lengthening contractions in mammalian skeletal muscle. *Muscle Nerve* 25:822–827, 2002.
10. Hameed, M., R. W. Orrell, M. Cobbold, G. Goldspink, and S. D. Harridge. Expression of IGF-I splice variants in young and old human skeletal muscle after high resistance exercise. *J. Physiol.* 547:247–254, 2003.
11. Hill, M., A. Wernig, and G. Goldspink. Muscle satellite (stem) cell activation during local tissue injury and repair. *J. Anat.* 203:89–99, 2003.

12. HUNTER, K. D., and J. A. FAULKNER. Pliometric contraction-induced injury of mouse skeletal muscle: effect of initial length. *J. Appl. Physiol.* 82:278–283, 1997.
13. KOH, T. J., J. M. PETERSON, F. X. PIZZA, and S. V. BROOKS. Passive stretches protect skeletal muscle of adult and old mice from lengthening contraction-induced injury. *J. Gerontol. A Biol. Sci. Med. Sci.* 58:592–597, 2003.
14. KOMI, P. V. Stretch-shortening cycle: a powerful model to study normal and fatigued muscle. *J. Biomech.* 33:1197–1206, 2000.
15. LEDVINA, M. A., and S. S. SEGAL. Sarcomere length and capillary curvature of rat hindlimb muscles in vivo. *J. Appl. Physiol.* 78: 2047–2051, 1995.
16. LOWE, W. L. Jr., S. R. LASKY, D. LEROITH, and C. T. ROBERTS, Jr. Distribution and regulation of rat insulin-like growth factor I messenger ribonucleic acids encoding alternative carboxyterminal E-peptides: evidence for differential processing and regulation in liver. *Mol. Endocrinol.* 2:528–535, 1988.
17. MAHONEY, D. J., K. CAREY, M. H. FU, et al. Real-time RT-PCR analysis of housekeeping genes in human skeletal muscle following acute exercise. *Physiol. Genomics* 18:226–231, 2004.
18. MCCULLY, K. K., and J. A. FAULKNER. Characteristics of lengthening contractions associated with injury to skeletal muscle fibers. *J. Appl. Physiol.* 61:293–299, 1986.
19. MCCULLY, K. K., and J. A. FAULKNER. Injury to skeletal muscle fibers of mice following lengthening contractions. *J. Appl. Physiol.* 59:119–126, 1985.
20. MCKOY, G., W. ASHLEY, J. MANDER, et al. Expression of insulin growth factor-1 splice variants and structural genes in rabbit skeletal muscle induced by stretch and stimulation. *J. Physiol.* 516:583–592, 1999.
21. OWINO, V., S. Y. YANG, and G. GOLDSPINK. Age-related loss of skeletal muscle function and the inability to express the autocrine form of insulin-like growth factor-1 (MGF) in response to mechanical overload. *FEBS Lett.* 505:259–263, 2001.
22. PIZZA, F. X. Muscle inflammatory cells after passive stretches, isometric contractions, and lengthening contractions. *J. Appl. Physiol.* 92:1873–1878, 2002.
23. ROBERTS, C. T. Jr., S. R. LASKY, W. L. LOWE, Jr., and D. LEROITH. Rat IGF-I cDNA's contain multiple 5-untranslated regions. *Biochem. Biophys. Res. Commun.* 146:1154–1159, 1987.
24. TORRELLA, J. R., J. M. WHITMORE, M. CASAS, V. FOUCES, and G. VISCOR. Capillarity, fibre types and fibre morphometry in different sampling sites across and along the tibialis anterior muscle of the rat. *Cells Tissues Organs* 167:153–162, 2000.
25. TOUMI, H., and T. M. BEST. The inflammatory response: friend or enemy for muscle injury? *Br. J. Sports Med.* 37:284–286, 2003.
26. UNDERWOOD, E. E. *Quantitative Stereology*, Reading, MA: Addison-Wesley Publishing Co., 1970.
27. WARREN, G. L., 3rd, J. H. WILLIAMS, C. W. WARD, et al. Decreased contraction economy in mouse EDL muscle injured by eccentric contractions. *J. Appl. Physiol.* 81:2555–2564, 1996.
28. WARREN, G. L., D. A. HAYES, D. A. LOWE, and R. B. ARMSTRONG. Mechanical factors in the initiation of eccentric contraction-induced injury in rat soleus muscle. *J. Physiol.* 464:457–475, 1993.
29. WARREN, G. L., D. A. HAYES, D. A. LOWE, B. M. PRIOR, and R. B. ARMSTRONG. Materials fatigue initiates eccentric contraction-induced injury in rat soleus muscle. *J. Physiol.* 464:477–489, 1993.
30. YANG, S., M. ALNAQEEB, H. SIMPSON, and G. GOLDSPINK. Cloning and characterization of an IGF-1 isoform expressed in skeletal muscle subjected to stretch. *J. Muscle Res. Cell. Motil.* 17: 487–495, 1996.